

Final Draft
of the original manuscript:

Alabbasi, A.; Mehjabeen, A.; Kannan, M.B.; Ye, Q.; Blawert, C.:
**Biodegradable polymer for sealing porous PEO layer on pure
magnesium: An in vitro degradation study**
In: Applied Surface Science (2014) Elsevier

DOI: 10.1016/j.apsusc.2014.02.100

Biodegradable polymer for sealing porous PEO layer on pure magnesium: An in vitro degradation study

Alyaa Alabbasi^a, Afrin Mehjabeen^a, M. Bobby Kannan^{a*}, Qingsong Ye^b, Carsten Blawert^c

^a*Biomaterials and Engineering Materials (BEM) Laboratory, ^bDiscipline of Dentistry,*

James Cook University, Townsville, Queensland 4811, Australia

^c*Magnesium Innovation Centre, Institute of Materials Research, Helmholtz-Zentrum*

Geesthacht, 21502 Geesthacht, Germany

ABSTRACT

An attempt was made to seal the porous silicate-based plasma electrolytic oxidation (PEO) layer on pure magnesium (Mg) with a biodegradable polymer, poly (L-lactide) (PLLA), to delay the localized degradation of magnesium-based implants in body fluid for better in-service mechanical integrity. Firstly, a silicate-based PEO coating on pure magnesium was performed using a pulsed constant current method. In order to seal the pores in the PEO layer, PLLA was coated using a two-step spin coating method. The performance of the PEO-PLLA Mg was evaluated using electrochemical impedance spectroscopy (EIS) and potentiodynamic polarization. The EIS results showed that the polarization resistance (R_p) of the PEO-PLLA Mg was close to two orders of magnitude higher than that of the PEO Mg. While the corrosion current density (i_{corr}) of the pure Mg was reduced by 65% with the PEO coating, the PEO-PLLA coating reduced the i_{corr} by almost 100%. As expected, the R_p of the PEO-PLLA Mg decreased with increase in exposure time. However, it was noted that the R_p

* Corresponding author. Tel.: +61 7 4781 5080; fax: +61 7 4781 6788.
E-mail address: bobby.mathan@jcu.edu.au (M.B. Kannan)

of the PEO-PLLA Mg even after 100 h was 6 times higher than that of the PEO Mg after 48 h exposure, and did not show any visible localized attack.

Key words: Magnesium; Biomaterial; Plasma electrolytic oxidation; Poly-L- lactide;

Degradation

1. Introduction

Interest in the use of ceramic coatings e.g., calcium phosphate and plasma electrolytic oxidation (PEO), on magnesium and magnesium-based alloys for producing high performance biodegradable implants has grown in recent years [1-5]. Generally, PEO coating technique, which has evolved from a traditional anodic oxidation process, provides a thick and adherent coating on metal substrates [6,7]. Recent studies have shown that PEO coatings on magnesium alloys have improved the corrosion resistance in chloride-containing solution [8] and also provide high wear resistant [9,10]. Unfortunately, the performance of PEO coatings on magnesium alloys deteriorates drastically under long-term exposure in aggressive environments such as in body fluid, i.e., the high chloride-containing electrolyte penetrates through the porous layer and rapidly breakdown the inner compact layer of PEO coating [11]. Hua et al. [12] reported that use of graphite to seal the porous layer of PEO coated pure aluminium has increased the degradation resistance significantly in chloride-containing solution. But for biodegradable biomaterials applications, the sealing material should be biocompatible and also biodegradable.

Biodegradable polymers such as poly (L- lactide) (PLLA), poly (glycolide) (PGA) and their co-polymers, which are popular in biomedical applications as biodegradable biomaterials, are candidate materials for sealing the pores of PEO coatings due to their biocompatibility [13,14] and also the slow degradation rate [15-17]. Recently, Lu et al. [18] studied the in vitro degradation behaviour of PLLA dip-coated on PEO coated WE42 Mg alloy. They reported

40% increase in the initial polarisation resistance (R_p) for the PEO-PLLA coated alloy as compared to that of the PEO coated Mg alloy. Generally, dip-coating method produces a relatively thick coating which might provide high initial resistance. However, long-term exposure of a thick coating can lead to peeling of the coating since the polymer (PLLA) undergoes bulk degradation [16]. It has been reported that spin-coating method can produce a thin and less porous coating than that of dip-coating method [19]. However, a one-step spin-coating method might not seal the pores in the PEO coating due to the complexity of the porous structure. Hence, in this study a two-step spin-coating of PLLA was attempted on a silicate-based PEO coating on pure Mg. A low-speed was used as the first step to allow the polymer to permeate through the pores, and then the second high-speed step was used to achieve a thin film on the PEO surface. The in vitro degradation behaviour of the PEO-PLLA coated samples was evaluated using electrochemical techniques in simulated body fluid (SBF).

2. Experimental Details

Pure Mg (99.9 wt. %) was used as a base material in this study. PEO coating was carried out in an electrolyte containing 2 g/l KOH and 7 g/l Na_2SiO_3 . A pulsed constant current method i.e., $30\text{mA}/\text{cm}^2$, 2 ms/18ms pulse on/off time, was applied for 20 min with a final voltage of $483 \pm 2\text{V}$. Further details on the PEO coating technique can be found elsewhere [20]. X-ray diffraction (XRD) analysis was performed using a Bruker X-ray diffractometer with $\text{Cu-K}\alpha$ radiation to determine the phase composition of the coating. Following the PEO coating, the samples were immersed in deionised boiling water for 90 min. PLLA (Poly (L-lactide), ester terminated RESOMER® L206 S (Aldrich) was dissolved in dichloromethane (DCM) 60% (w/v) and applied on the PEO coating using a VTC spin coater. The spin coating was conducted in two steps, i.e., firstly a small amount of polymer solution was placed on the PEO surface of the

sample and then spin coated at 500 rpm for 10 sec, and the second step coating was done at a rotational speed of 2000 rpm for 10 sec. A lower rotation speed coating was chosen for the first-step coating in order to seal the pores, and the second-step coating was at a higher speed to create a uniform coating on the surface. The coating thickness was measured using a coating thickness gauge (DualScope®, Fischer, Germany).

In vitro degradation studies were carried out in simulated body fluid (SBF) maintained at a physiological pH value of 7.4 and temperature of $37\pm 0.5^{\circ}\text{C}$. All the experiments were conducted in triplicate. The composition of the SBF is shown in Table 1. The SBF was buffered with tris (hydroxymethyl) aminomethane (TRIS) to maintain a physiological pH of 7.4. A standard three electrode system, was used for the electrochemical tests i.e., a sample (0.785 cm^2 exposed area) as a working electrode, Ag/AgCl (saturated KCl) as a reference electrode and a graphite rod as a counter electrode. Measurements were taken using a VersaSTAT3 (PAR) potentiostat and a frequency response analyser. Electrochemical impedance spectroscopy (EIS) experiments were performed at the open circuit potential with AC amplitude of 5 mV over the frequency range of 10^5 Hz to 10^{-2} Hz . The EIS plots were modelled using ZSimpWin 3.21 software (Princeton Applied Research, US). Prior to the beginning of the electrochemical experiments, the samples were kept immersed in the SBF for 2 h.

3. Results and discussion

Fig.1. shows the XRD pattern for the PEO coating, which suggests that the coating mainly consists of MgO and Mg_2SiO_4 . The morphology of the coating is shown in Fig. 2(a, b). Fig 2(a) reveals a typical porous structure of PEO coating. A few cracks can also be noticed in Fig 2(b), indicating the brittleness of the coating. The thickness of the PEO coating was $24\pm 3\text{ }\mu\text{m}$, and after spin-coating of PLLA, the total coating thickness was $33\pm 2\text{ }\mu\text{m}$.

The Nyquist plots for the pure Mg and the coated samples after 2 h exposure in SBF are shown in Fig. 3. The pure Mg shows two capacitive loops and one inductive loop. In contrast to the pure Mg, the PEO coated samples showed only one large capacitive loop. Interestingly, the PEO-PLLA coated samples showed two large capacitive loops, however there was no inductive loop. An equivalent circuit model i.e. $R(Q(R(QR)))$, was used to analyse the impedance data. This model has been used for bare Mg [21], PEO coated samples [3, 20,22] and double-layered coated samples [23]. Although the same equivalent circuit was used for the bare metal and the coated samples, the physical process represented by the circuit elements are different. For pure Mg, R_1 represents the charge transfer resistance, CPE_1 the double layer capacitance; R_2 and CPE_2 represent the film effects. For the PEO coated sample, R_1 and CPE_1 represent the outer porous layer, R_2 and CPE_2 represent the resistance of the compact inner layer. For PEO-PLLA coated sample R_1 and CPE_1 represent the resistance of PLLA, R_2 and CPE_2 represent the resistance of the PEO layer. The polarisation resistance (R_p) was calculated by adding R_1 and R_2 . The obtained results from the EIS modelling are shown in Table 2. The PEO coated samples showed close to an order of magnitude higher R_p than the pure Mg. Importantly, the PEO-PLLA coated samples showed close to three orders of magnitude higher R_p than the pure Mg and was close to two orders of magnitude higher R_p than the PEO coated samples. The R_p values were $470 \Omega.cm^2$, $4300 \Omega.cm^2$, and $1.18 \times 10^5 \Omega.cm^2$ for the pure Mg, the PEO coated and the PEO-PLLA coated samples, respectively. For both the PEO and the PEO-PLLA coated samples, the R_2 is significantly higher as compared with R_1 , which indicates that the R_p for both the coatings depend on the inner layer resistance. The polarisation curves for the pure Mg, the PEO coated and the PEO-PLLA coated samples are shown in Fig. 4 and the corresponding electrochemical data are presented in Table 3. The E_{corr} of the PEO-PLLA coated samples was shifted by $\sim 250mV$ toward the noble direction as compared to that of the pure Mg, whereas the PEO coated samples showed $\sim 100mV$ shift

towards the active direction. The corrosion current density (i_{corr}) calculated based on the cathodic curves showed that the i_{corr} of the pure Mg was reduced by 65% with the PEO coating and almost by 100% with the PEO-PLLA coating.

Long-term in vitro degradation studies were performed on the bare metal and the coated samples. It should be noted that the SBF was changed after every 24 h exposure to maintain the pH at 7.4. The R_p values for the samples at different exposure times in SBF are shown in Fig. 5. As the R_p of pure Mg remained relatively stable at a low value ($\sim 1000 \Omega \cdot \text{cm}^2$), the R_p of the PEO coated samples decreased by 80% after 48h, from $4300 \Omega \cdot \text{cm}^2$ to $900 \Omega \cdot \text{cm}^2$. The drop in the R_p values suggests that the electrolyte has penetrated through the porous layer and attacked the base metal. Since the R_p of both bare metal and the PEO coated samples were similar and low after 48 h exposure, the experiments for these samples were stopped after 48 h.

The PEO-PLLA coated samples also showed a drop in the R_p value after 24 h exposure, however the R_p was more than one order of magnitude higher than that of the pure magnesium and the PEO coated samples. The decrease in the R_p of the PEO-PLLA coated samples could be attributed to the bulk degradation mechanism of PLLA [24]. It can be noted that the R_p value of the PEO-PLLA samples even after 100 h exposure was $5.4 \times 10^3 \Omega \cdot \text{cm}^2$, which is still significantly higher than the PEO coated samples measured after 48 h. The results suggest that the PLLA coating has filled the porous of the PEO layer and prevented the penetration of the electrolyte and as a result the PEO-PLLA coated samples showed higher R_p than the PEO coated samples throughout the tests. Interestingly, the R_p reported by Lu et al. [18] for a PEO-PLA coated alloy was higher than that observed in this study. This could be due to the difference in the pH condition of the electrolyte during the experiments. If the electrolyte is not changed regularly during the long-term experiments, which was the case in Lu et. al.[18] work, the pH of the electrolyte will increase and as a

consequence Mg passivates and the R_p would not change significantly or it might even increase. Hence, it is critical to change the SBF regularly during the long-term testing to maintain the pH of the electrolyte to mimic the physiological condition.

Fig. 6 shows the post-degradation photographs of the pure Mg and the coated samples. The pure Mg has undergone high degradation after 48 h exposure to SBF. High localized degradation is readily seen in the photograph of the pure Mg. The PEO coated samples showed no high localized degradation, but a few patches of localized attack were observed. In contrast to the pure Mg and PEO coated samples, the PEO-PLLA coated samples showed no sign of localized degradation.

The degradation mechanisms of the pure Mg, the PEO coated and the PEO-PLLA coated samples are schematically shown in Fig. 7. It is well known that high-chloride concentration, as in the SBF, causes high localized degradation in pure magnesium [25]. The native film (MgO) and the degradation product film, $Mg(OH)_2$, formed in aqueous solution are not protective in chloride-containing solution [26], and as a result a high level of localized degradation was observed within 48 h of exposure to SBF. The PEO coating did show some protection against degradation during the initial exposure period of sample. However, the porous nature of the outer film has paved way for the chloride ions to penetrate through and dissolve the inner layer, which led to localized degradation after a period of exposure to SBF. The double layer coating (PEO-PLLA) has shown a significant improvement in the degradation resistance under short-term exposure. The polymer top layer has acted as a protective barrier and largely inhibited the penetration of the electrolyte. With exposure time, the polymer dissolution occurred and as a result of the bulk degradation mechanism of PLLA, the electrolyte has reached the porous layer and the base metal and hence the resistance has decreased. However, a the penetration of the electrolyte appears to be minimal since the R_p

was significantly high even after 100 h exposure. It is important to note that there was no sign of localized degradation even after 100 h of exposure to SBF.

4. Conclusions

The study showed that PLLA coating on PEO coated magnesium is highly beneficial for improving the localized degradation resistance for potential load-bearing implant applications. The PEO-PLLA coated alloy did not show any sign of localized degradation even after 100 h exposure to SBF, while the PEO coated magnesium exhibited localized attack after 48 h exposure. In vivo studies should be carried out to confirm the effectiveness of the coating.

References

- [1] M. B. Kannan and L. Orr, In vitro mechanical integrity of hydroxyapatite coated magnesium alloy, *Biomedical Materials* 6 (2011) 045003 (11pp).
- [2] M. B. Kannan, Enhancing the performance of calcium phosphate coating on a magnesium alloy for bioimplant applications, *Material Letters* 76(2012) 109-112.
- [3] A. Alabbasi , M. B. Kannan , R.Walter , M.Störmer , C.Blawert, Performance of pulsed constant current silicate-based PEO coating on pure magnesium in simulated body fluid , *Material Letters* 106 (2013) 18-21.
- [4] M. B. Kannan, O. Wallipa, Potentiostatic pulse-deposition of calcium phosphate on magnesium alloy for temporary implant applications — An in vitro corrosion study, *Material Science & Engineering C33* (2013) 675-679.
- [5] Y. Harada, S. Kumai, Effect of ceramics coating using sol–gel processing on corrosion resistance and age hardening of AZ80 magnesium alloy substrate, *Surface Coating & Technology* 228 (2013) 59-67

- [6] A.L. Yerokhin, X. Nie, A. Leyland, A. Matthews, S.J. Dowey, Plasma electrolysis for surface engineering, *Surface Coating & Technology* 122 (1999) 73-93.
- [7] J. Cai, F. Cao, L. Chang, J. Zheng, J. Zhang, C. Cao, The preparation and corrosion behaviors of MAO coating on AZ91D with rare earth conversion precursor film, *Applied Surface Science* 257 (2011) 3804-3811
- [8] H. Guo, M. An, S. Xu, H. Huo, Microarc oxidation of corrosion resistant ceramic coating on magnesium alloy, *Materials Letters* 60 (2006) 1538-1541
- [9] G. Rapheal, S. Kumar, C. Blawert, Narendra B. Dahotre, Wear behavior of plasma electrolytic oxidation (PEO) and hybrid coatings of PEO and laser on MRI 230D magnesium alloy, *Wear* 271 (2011) 1987-1997.
- [10] S. Durdu, M. Usta, Characterization and mechanical properties of coatings on magnesium by micro arc oxidation, *Applied Surface Science* 261 (2012) 774-782
- [11] J. Liang, P. B. Srinivasan, C. Blawert, W. Dietzel, Influence of chloride ion concentration on the electrochemical corrosion behavior of plasma electrolytic oxidation coated AM50 magnesium alloy, *Electrochimica Acta* 55 (2010) 6802-6811.
- [12] L. G. Hua, C. Huan, W. X. Quan, P. Hua, Z.G. Ling, Z. Bin, L.H. Ju, Y. Si-Ze, Characteristics of sealed plasma electrolytic oxidation coatings with electrochemical impedance spectroscopy, *Chin. Phys B* 19 (2010) 085202.
- [13] Ivan K. De Scheerder, Krzysztof L. Wilczek, Eric V. Verbeken, Joke Vandorpec, Pham N. Lan, Etienne Schacht, Hilaire De Geest, Jan Piessens, Biocompatibility of polymer-coated oversized metallic stents implanted in normal porcine coronary arteries, *Atherosclerosis* 114 (1995) 105-114
- [14] A.A. Ignatius and LX. Claes, In vitro biocompatibility of bioresorbable polymers: poly(DLlactide) and poly(L-lactide-co-glycolide), *Biomaterials* 17 (1996) 631-639.

- [15] E. Veya, C. Rogerb, L. Meehanb, J. Boothb, M. Claybournb, A. F. Miller, A. Saiani , Degradation mechanism of poly(lactic-co-glycolic) acid block copolymer cast films in phosphate buffer solution, *Polymer Degradation and Stability* 93 (2008) 1869–1876
- [16] A. Alabbasi, S. Liyanaarachchi, M. B. Kannan, Polylactic acid coating on a biodegradable magnesium alloy: An in vitro degradation study by electrochemical impedance spectroscopy, *Thin Solid Films* 520 (2012) 6841-6844.
- [17] M. B. Kannan, S. Liyanaarachchi, Hybrid coating on a magnesium alloy for minimizing the localized degradation for load-bearing biodegradable mini-implant applications, *Materials Chemistry and Physics* 142 (2013) 1-5.
- [18] P. Lu, L. Cao, X. Xu, X. Wu X, Evaluation of magnesium ions release, biocorrosion, and hemocompatibility of MAO/PLLA-modified magnesium alloy WE42. *Biomedical Materials Research* 96B (2011) 101-109.
- [19] J. Hong, H. Park, Fabrication and characterization of block copolymer micelle multilayer films prepared using dip-, spin- and spray-assisted layer -by-layer assembly deposition, *Colloids and Surface A: Physicochem. Eng. Aspects.* 381 (2011) 7-12.
- [20] J. Liang, P.B. Srinivasan, C. Blawert, M. Störmer, W. Dietzel, Electrochemical corrosion behaviour of plasma electrolytic oxidation coatings on AM50 magnesium alloy formed in silicate and phosphate based electrolytes, *Electrochimica Acta* 54 (2009) 3842-3850.
- [21] R. Walter, M. B. Kannan, In-vitro degradation behaviour of WE54 magnesium alloy in simulated body fluid, *Materials Letters* 65 (2011) 748-750.
- [22] A. Ghasemi, V.S. Raja, C. Blawert, W. Dietzel, K.U. Kainer, Study of the structure and corrosion behaviour of PEO coatings on AM50 magnesium alloy by electrochemical impedance spectroscopy, *Surface & Coating Technology* 202 (2008) 3513-3518.

- [23] L. Zeng, S. Yang, W. Zhang, Y. Guo, C. Yan, Preparation and characterization of a double-layer coating on magnesium alloy AZ91D, *Electrochimica Acta* 55 (2010) 3376-3383.
- [24] X. Zhang, U.P. Wyss, D. Pichora, M.F.A. Goosen, An Investigation of Poly(lactic acid) Degradation, *Journal of Bioactive and Compatible Polymers* 9 (1994)80.
- [25] M. B. Kannan, Influence of microstructure on the in-vitro degradation behaviour of magnesium alloys, *Materials Letters* 64 (2010) 739-742.
- [26] G. Song G, A. Atrens A, Understanding magnesium corrosion, *Advanced Engineering Materials* 5 (2003), 837-858.

TABLES

Table 1

Chemical composition of the simulated body fluid (SBF)

Reagent	Amount
NaCl (g/L)	8.036
NaHCO ₃ (g/L)	0.352
KCl (g/L)	0.225
K ₂ HPO ₄ ·3H ₂ O(g/L)	0.230
MgCl ₂ ·6H ₂ O (g/L)	0.311
1.0 M HCl (mL/L)	40
CaCl ₂ (g/L)	0.293
Na ₂ SO ₄ (g/L)	0.072
TRIS buffer (g/L)	6.063

Table 2

EIS fitting results for the pure magnesium, PEO coated and PEO-PLLA coated samples exposed for 2 h in SBF.

Sample	CPE ₁ ($\Omega^{-1} \cdot \text{cm}^{-2} \cdot \text{s}^{-n}$)	n	R ₁ ($\Omega \cdot \text{cm}^2$)	CPE ₂ ($\Omega^{-1} \cdot \text{cm}^{-2} \cdot \text{s}^{-n}$)	n	R ₂ ($\Omega \cdot \text{cm}^2$)	R _p ($\Omega \cdot \text{cm}^2$)
Pure Mg	4.8 (0.3)×10 ⁻⁵	0.82	411 (72.7)	2.9 (0.2)×10 ⁻³	0.98	56.92 (0.59)	470 (72)
PEO	1.06 (0.4)×10 ⁻⁸	0.98	88.2 (2.6)	6.2 (1.7)×10 ⁻⁶	0.72	4211 (147)	4300 (150)
PEO+PLLA	1.31 (1.05)×10 ⁻⁶	0.61	1544 (339)	4.2 (3.9)×10 ⁻⁷	0.81	117000 (28545)	118544 (26319)

Note: All experiments were conducted in triplicate and the standard deviations are provided in brackets.

Table 3

Electrochemical degradation data for pure magnesium, PEO coated and PEO-PLLA coated samples from potentiodynamic polarisation curves.

Sample	E_{corr} (V _(Ag/AgCl))	i_{corr} ($\mu\text{A}/\text{cm}^2$)
Pure Mg	-1.8 (0.02)	23.5 (3.6)
PEO	-1.92 (0.02)	8.3 (3)
PEO-PLLA	-1.54 (0.01)	0.03 (0.2)

Note: All experiments were conducted in triplicate and the standard deviations are provided in brackets.

FIGURE CAPTIONS

Fig. 1. XRD spectra of PEO coated Mg sample.

Fig. 2. SEM micrographs of PEO coated Mg sample.

Fig. 3. Nyquist plots of (a) pure Mg and PEO coated sample, and (b) PEO-PLLA coated sample, after 2 h immersion in SBF.

Fig. 4. Potentiodynamic polarisation curves of pure Mg, PEO coated and PEO-PLLA coated samples after 2 h immersion in SBF.

Fig. 5. Polarization resistance (R_p) of pure Mg, PEO coated and PEO-PLLA coated samples after different immersion intervals in SBF.

Fig. 6. Photographs of pure Mg and PEO coated sample after 48 h exposure in SBF, and PEO-PLLA coated sample after 100 h exposure in SBF.

Fig. 7. Schematic representation of the in vitro degradation processes of pure Mg, PEO coated and PEO-PLLA coated samples.

Fig.1
[Click here to download high resolution image](#)

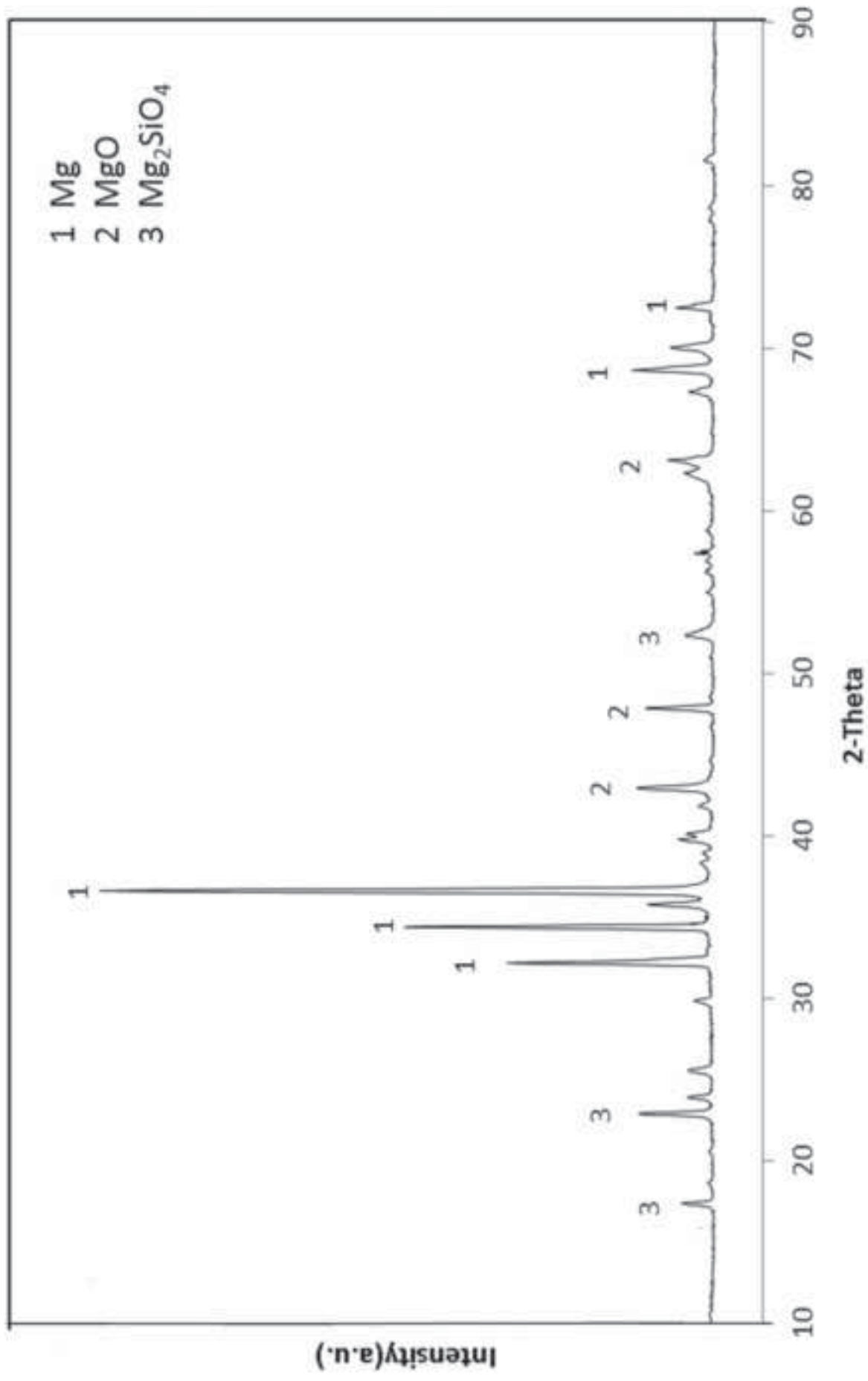
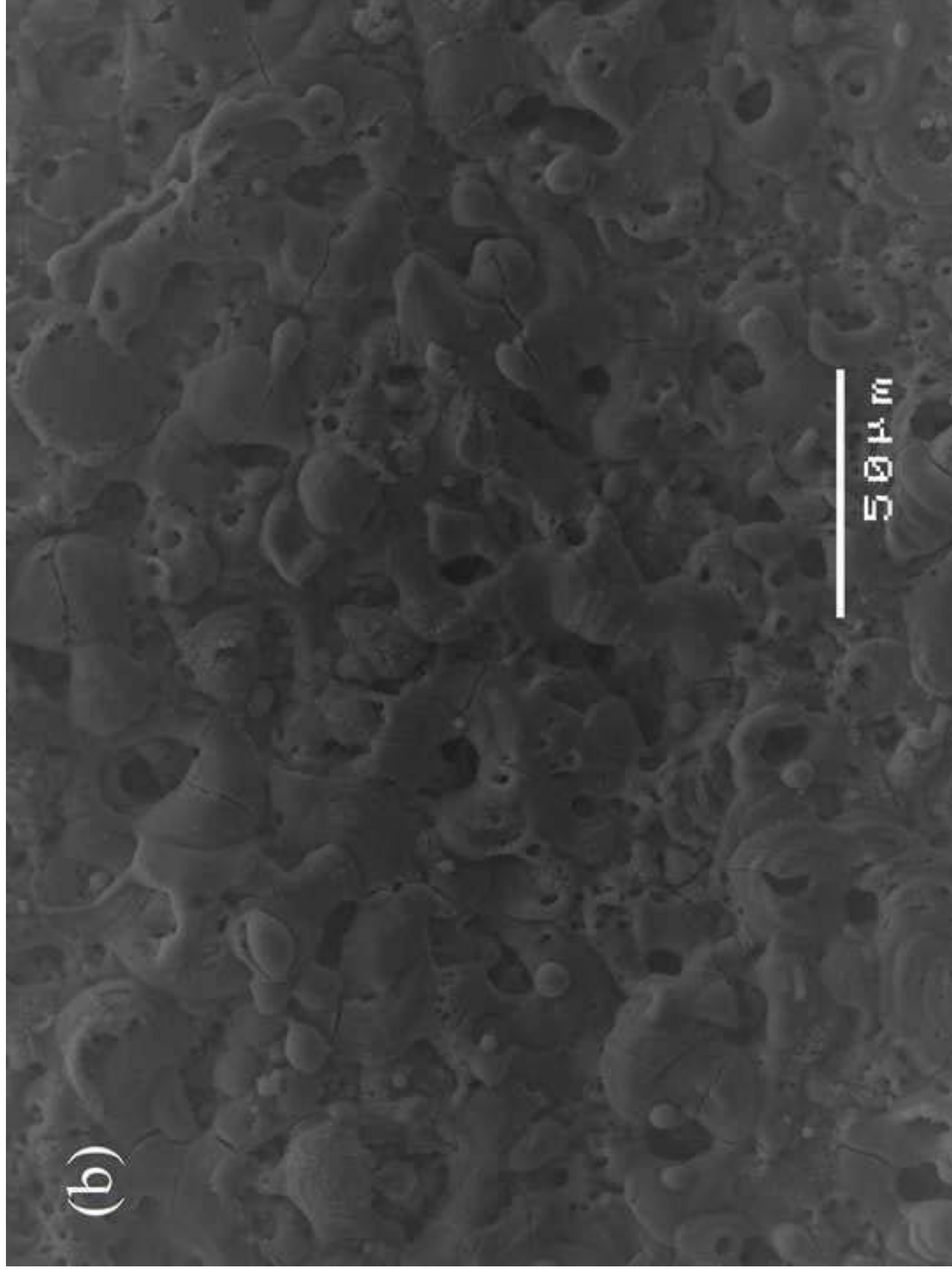


Fig.2a
[Click here to download high resolution image](#)



Fig.2b
[Click here to download high resolution image](#)



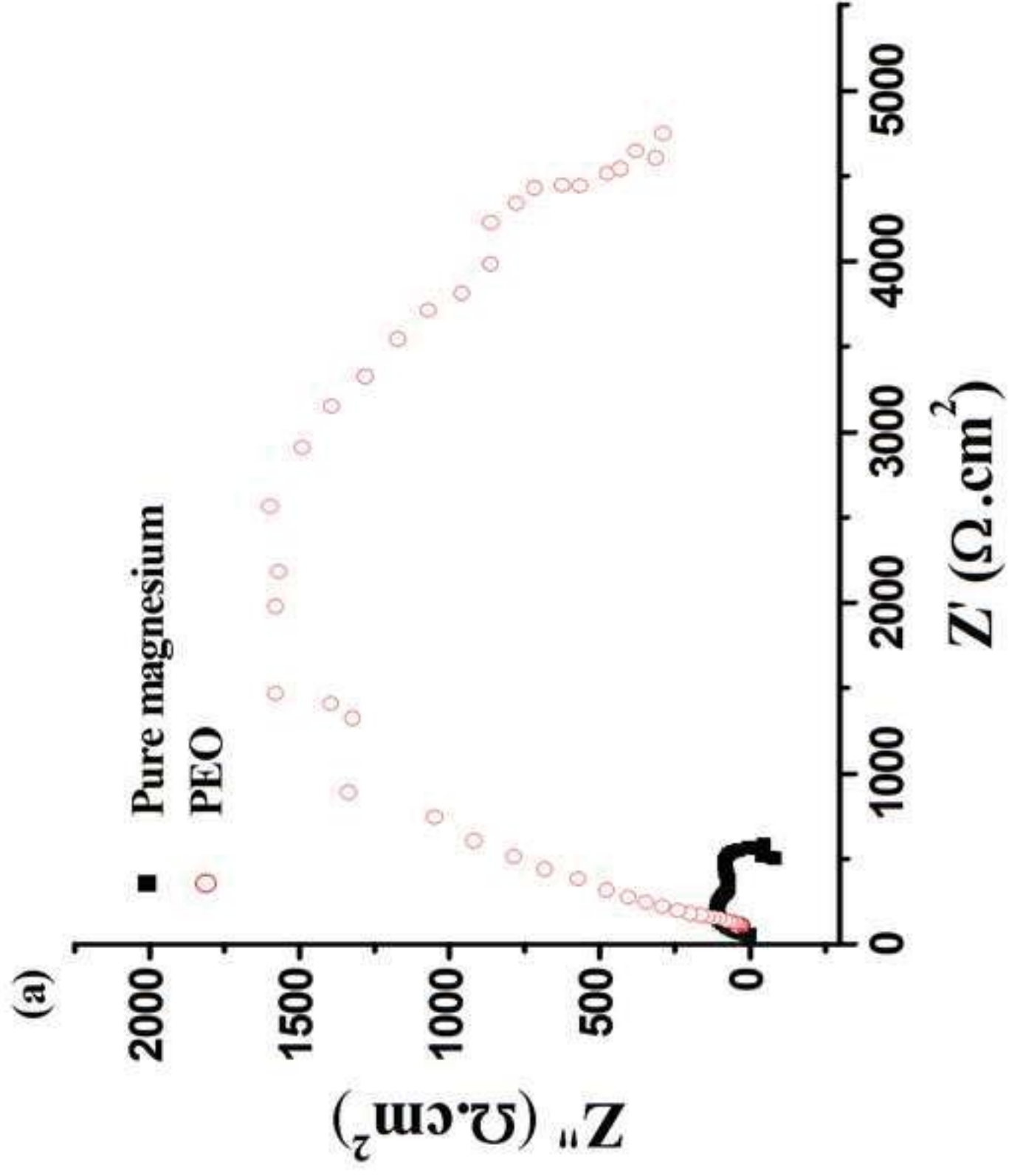


Fig.3b
[Click here to download high resolution image](#)

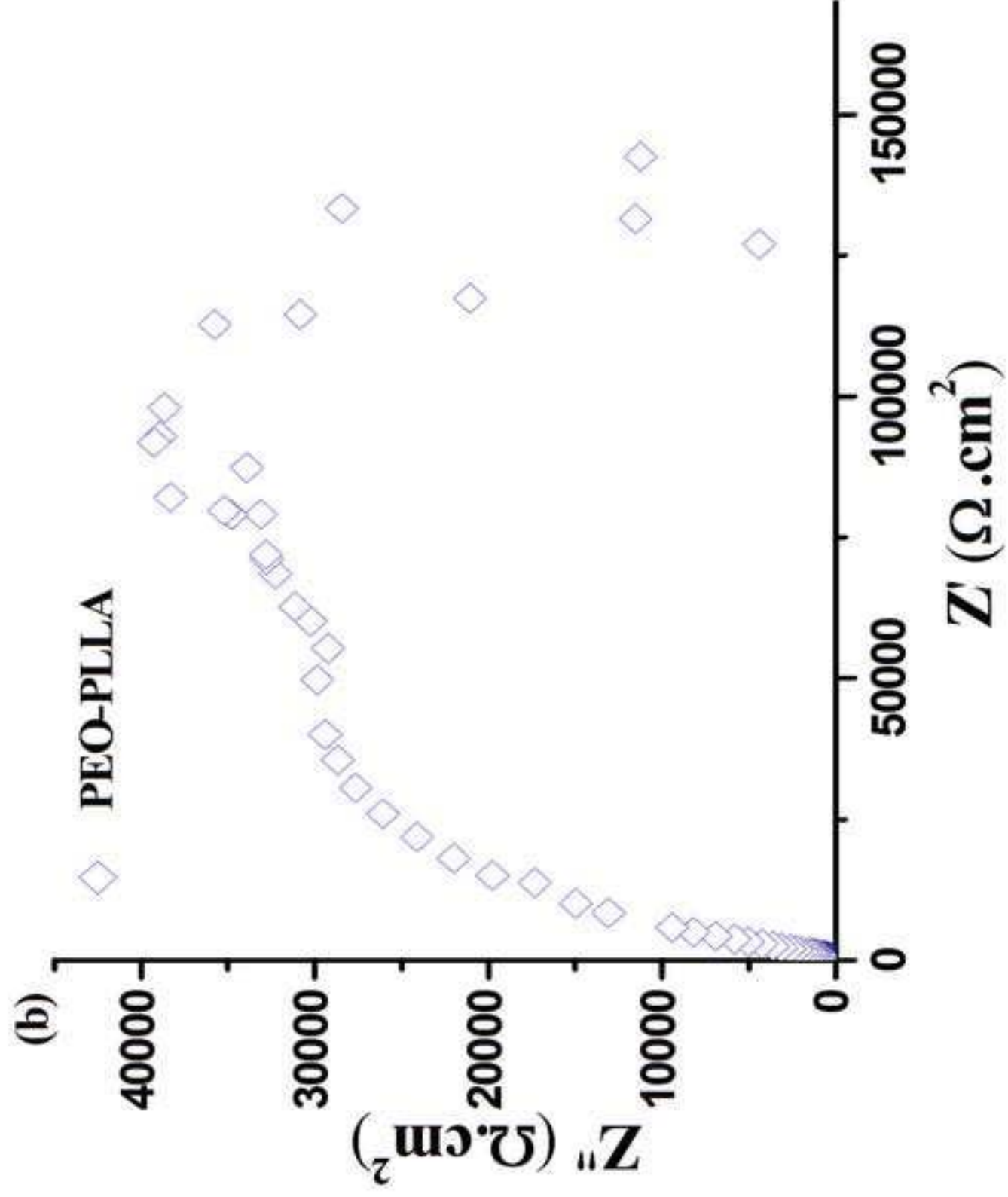


Fig.4
[Click here to download high resolution image](#)

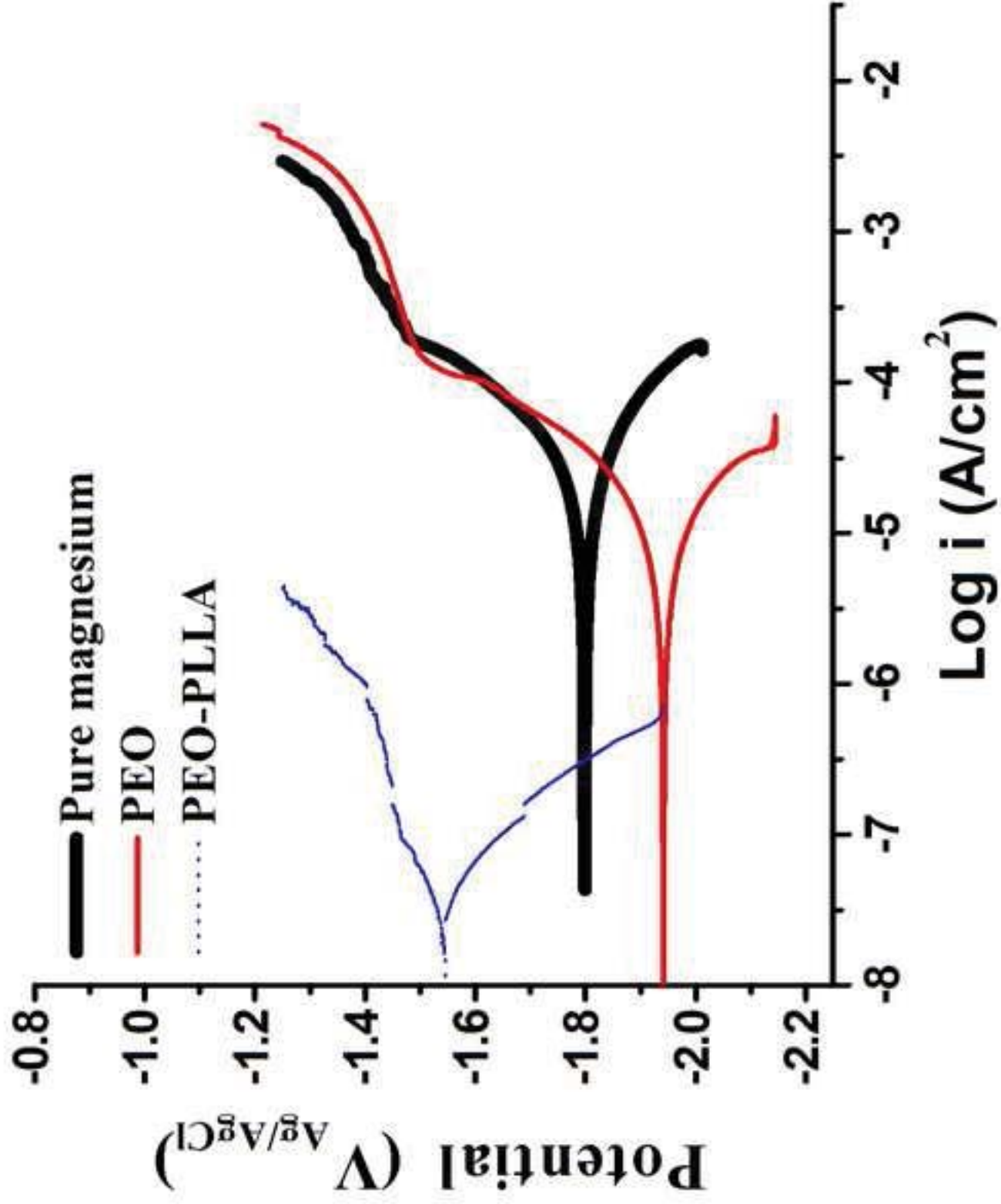
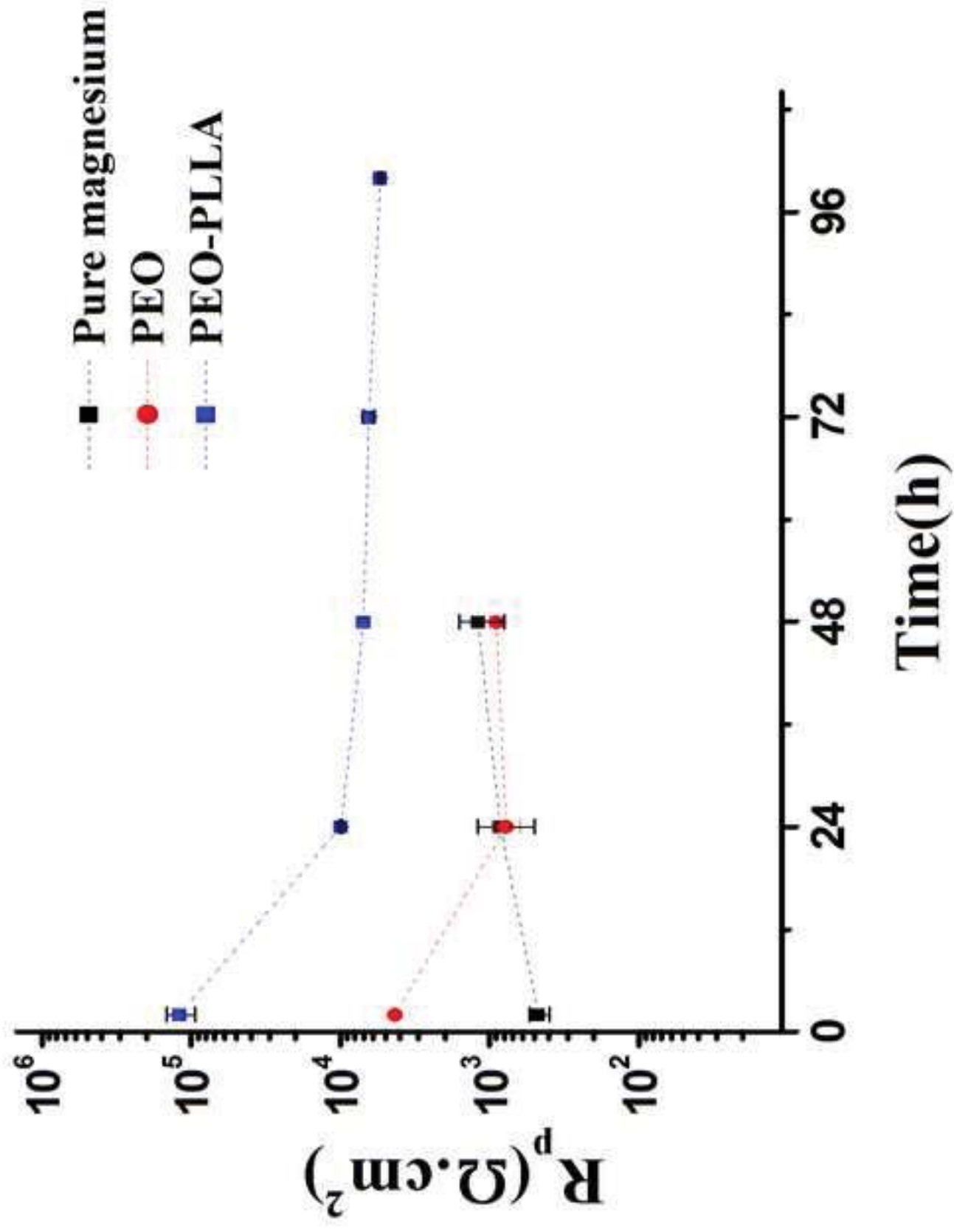


Fig.5
[Click here to download high resolution image](#)



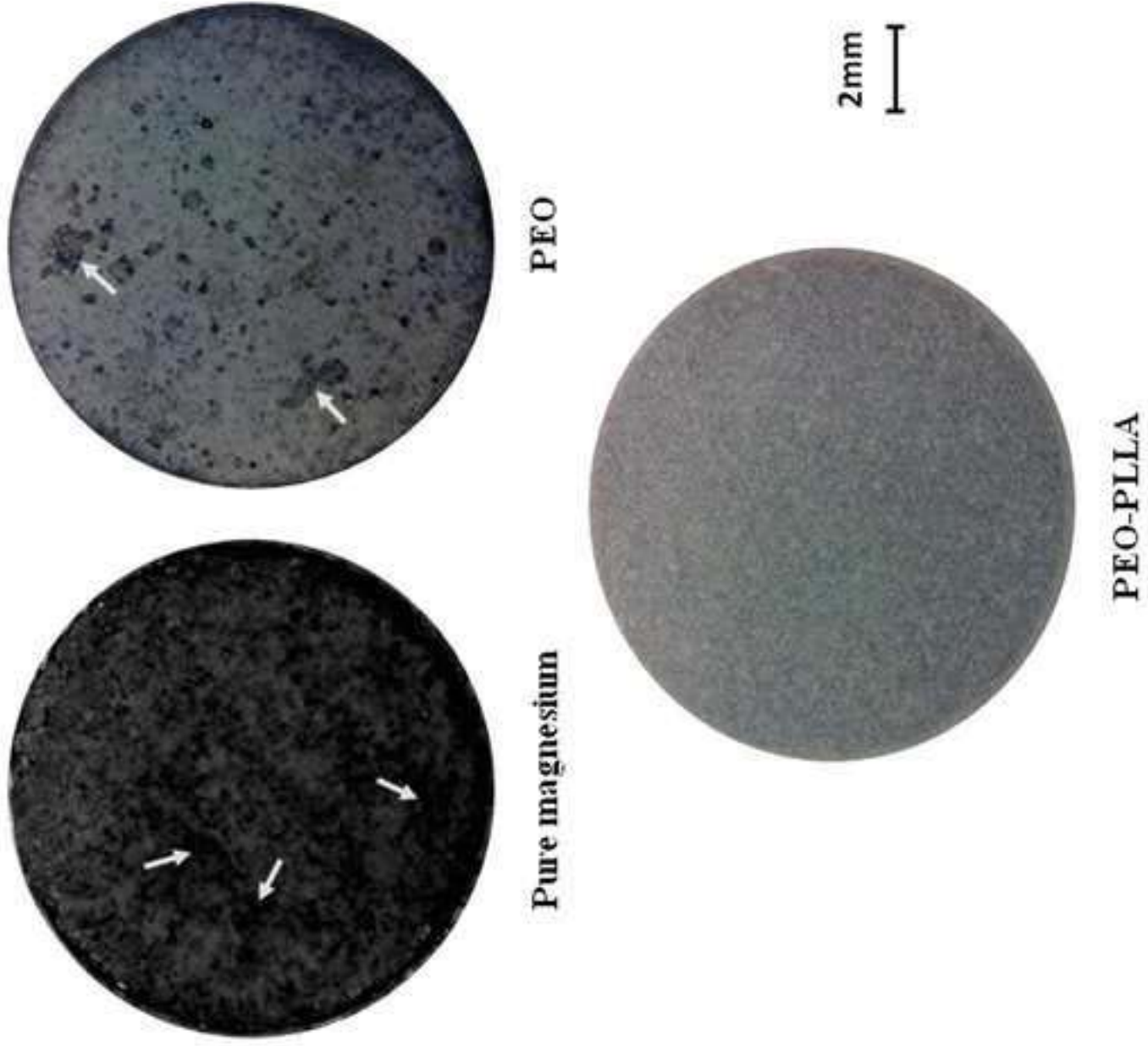


Fig.7
[Click here to download high resolution image](#)

